Alteration zonation in the Loma Blanca kaolin deposit, Los Menucos, Province of Rio Negro, Argentina

Presented at the XIV International Clay Conference, Castellaneta Marina, Italy, June 2009

S. A. MARFIL[1,2,*], P. J MAIZA[1,3] AND N. MONTECCHIARI[1]

[1] *Department of Geology – INGEOSUR, Universidad Nacional del Sur, San Juan 670, 8000 Bahía Blanca, Argentina,*
[2] *Independent Researcher at CIC de la Provincia de Buenos Aires, Argentina, and* [3] *Principal Researcher at CONICET. Argentina*

ABSTRACT: The Loma Blanca mine is in one of the northwest kaolinized zones of the Los Menucos area (Patagonia, Argentina). The parent rocks are andesites and andesitic tuffs from the Vera Formation, Los Menucos Group (Lower Triassic). Hayase & Maiza (1974) proposed a concentric zonation model. From the parent rock outward, four different alteration patterns were recognized: Zone 1, with sericite, chlorite and montmorillonite; Zone 2, with kaolinite and dickite; Zone 3, with dickite, pyrophyllite and alunite; and Zone 4, with quartz, disseminated sulphides and diaspore.

The relationship between the chemical composition of major, minor and trace elements and the mineralogical alteration zonation was evaluated to confirm the genesis of the deposit. Fe_2O_3, CaO, Na_2O and K_2O contents decrease from Zone 1 to Zone 3, whereas Al_2O_3 and LOI increase in the kaolinite-alunite zone. In the chemical composition of alunite, Na > K. Large Ba, Sr, V and Zr contents were observed mainly in Zones 2 and 3. Co, Ni, Cu, Zn and Rb are more common in Zone 1. *LREE* are more abundant than *HREE* in Zones 2 and 3. In kaolinites $\delta^{18}O$ values range from 10.8‰ to 13.2‰, and δD from −83‰ to −85‰.

The mineral assemblage (dickite-alunite-pyrophyllite-diaspore), the alteration zonation pattern (laterally concentric), the geochemistry of trace elements, the relation between *LREE* and *HREE* and the small $\delta^{18}O$ values suggest that the Loma Blanca deposit was formed by hydrothermal processes.

KEYWORDS: geochemistry, kaolin, chlorite, kaolinite, dickite, pyrophyllite, Loma Blanca deposit, Argentina.

In the province of Río Negro (Patagonia, Argentina) there are a large number of kaolin deposits hosted by volcanic rocks of the Los Menucos Group. The sequence starts with andesitic volcanism and ends with rhyolitic pyroclastic facies. Most of the kaolin deposits are hosted by rhyolitic tuffs (Sierra Colorada Formation) of Upper Triassic to Middle Jurassic age. These mines have been extensively studied (Maiza, 1972; Maiza & Mas, 1981; Marfil *et al.*, 2000; and Maiza *et al.*, 2003). Loma Blanca is one of the northernmost kaolinized zones in the area and is the only deposit hosted by andesitic rocks.

Terakado & Fujitani (1998) studied the rare earth elements and other trace elements in silicastones, alunites and related rocks in order to examine the behaviour of trace elements in the acidic hydrothermal alteration of silicic volcanic rocks. They found that most of the elements such as Na, Fe, Ba

* E-mail: smarfil@uns.edu.ar

and *LREE* were leached from the silicastones, while *HREE*, Th, Hf and Zr were retained in the rocks, even under strongly acidic hydrothermal processes. Alunite samples have *LREE*-enriched and *HREE*-depleted features.

According to Dill *et al.* (1997), the ratios TiO_2 + Fe_2O_3 *vs.* Cr + Nb, Zr *vs.* TiO_2 and Ba + Sr *vs.* Ce + Y + La in kaolinites allow discrimination between hypogene and supergene kaolinization processes. The APS-bearing argillaceous zones that formed during supergene processes are significantly enriched in *REE* relative to hypogene equivalents (Dill, 2001).

Pandarinath *et al.* (2008) studied the effects of hydrothermal alteration on major, rare-earth, and other trace-element concentrations in rhyolitic rocks of the Los Azufres geothermal field, Mexico. They concluded that the hydrothermal alteration resulted in a decrease in MnO, P_2O_5, Ta, Rb/Zr and Rb/Nb, and an increase in Zr, Nb and Nb/Y. The greater variances of several chemical variables in altered rocks (Y, Ce, Pr, Nd, Sm, Lu and Pb) are probably due to hydrothermal processes, whereas smaller variances of other altered rock variables (CaO, Sr, Rb/Sr and Rb/Ba) suggest that these processes led to more uniform chemical rock compositions. The concentrations of *REE* were not significantly different between fresh and altered rhyolitic rocks, which implies that either these elements remained immobile or were reincorporated into secondary minerals during the hydrothermal alteration of the rhyolitic rocks.

Papoulis & Tsolis-Katagas (2008) studied kaolin deposits in the western and southern parts of Limnos Island, northeast Aegean Sea, Greece, and they found four types of hydrothermal alteration zones: smectite-illite-halloysite and kaolinite-dickite-rich zones. Mineral assemblages reveal that temperatures ranged from <100ºC (smectite-rich and halloysite-rich zones) to ~270ºC (kaolinite-dickite-rich zones). Limited supergene alteration was observed in the less hydrothermally altered rocks of the illite-rich zones as suggested by the presence of jarosite and pyrite. The development of the various assemblages depends not only on the temperature and composition of the hydrothermal fluids but also on the distance of the rock from the fault or the channel of the ascending hydrothermal fluids.

Papoulis *et al.* (2004) used the K and Na content in a kaolin deposit from Greece to measure the degree of alteration of primary rocks. The positive correlation between Al_2O_3 and LOI and the large negative loadings between $SiO_2-Al_2O_3$ and SiO_2-LOI indicate that LOI and Al_2O_3 contents increase in the more altered samples.

Ece *et al.* (2008) studied acid-sulphate hydrothermal alteration in andesitic tuffs in the Biga Peninsula (Turkey) and concluded that the changes in the chemical composition of geothermal waters through time and the chemistry of the intermediate products in clay deposits also control the formation of alunite. The main geothermal activity and acid-sulphate alterations for the mineralizations of alunite and halloysite occurred after the onset of NAF-related faulting in the Biga Peninsula. The P_2O_5 enrichment in alunite nodules suggests a deep magmatic source for the geothermal waters that passed through the shallow-level granodiorite intrusions.

The aim of the work described in this paper was to evaluate the relation between the chemical composition of major, minor and trace elements, the stable isotopes in kaolin (O and D) and the mineralogical alteration zonation to confirm the genesis of the deposit.

GEOLOGICAL SETTING AND MINERALOGY

Loma Blanca is situated 70 km NW of Los Menucos (Río Negro Province, Argentina) (Fig. 1). The parent rocks are andesites and their tuffs from the Vera Formation (Lower Triassic) (Los Menucos Group), which lie unconformably on the La Esperanza granite and Colo Niyeu methamorphites. 150 m to the northeast of the deposit there is an outcrop of granite intruded by aplitic dykes. Its geological importance arises from the mineralogy, structure and setting of the strongly mineralized area and its relationship with the different lithologic units.

Hayase & Maiza (1974) studied the mineralogy of the Loma Blanca deposit using XRD, TG, DTA and microscopy. They concluded that the deposit was formed by the activity of an acid hydrothermal solution or superheated solfatara. They proposed a concentric zonation model. From the parent rock outward, different alteration patterns were recognized: a zone with sericite, chlorite and montmorillonite; a zone with kaolinite and dickite; a zone with dickite, pyrophyllite and alunite-natro-alunite; and a zone with quartz, disseminated sulphides and diaspore (Fig. 2).
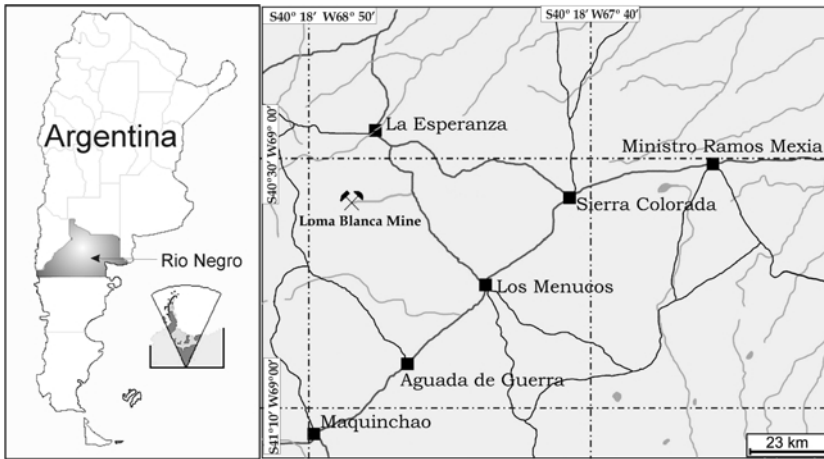
Fig. 1. Location of the Loma Blanca mine.

The structure is not clearly exposed due to the scarce outcrops and smooth geomorphical topography covered by recent sediments. Geological evidence from the area indicates the development of tectonic fracturing and differential block movements affecting the heterogeneous volcanosedimentary pile that channelled the hydrothermal solutions responsible for the mineralization. The mineral assemblage, with high-temperature minerals (diaspore, pyrophyllite and dickite), the abovementioned sulphides, the areal structure and favourable lithology related to mineralization processes identify this zone as suitable for metallic mineral prospecting.

The floor of the Loma Blanca mine consists of andesite that shows progressive alteration and development of a propylitic zone. Tuffaceous levels are transitionally interlayered; they are affected by tectonics and have developed breccia zones that, owing to their greater permeability, provide pathways for mineralizing solutions. Towards the top of the mineralized zone, the texture is obliterated due to the intense silicification that has erased the lithological characteristics of the affected rocks (Maiza *et al.*, 2009).

The oldest formation in the area is Colo Niyeu, which is a low-grade metasedimentary basement. According to Labudia & Bjerg (1994), it could only be assigned a pre-Permian age. This unit was intruded by different plutonites of the so-called Complejo Plutónico La Esperanza. Close to the deposit, outcrops attributed to the Donosa granite, due to their mineralogical and textural characteristics, were recognized; the age of the intrusion, according to Pankurst *et al.* (1992), will be Late Permian. Over these formations lie the lithologic
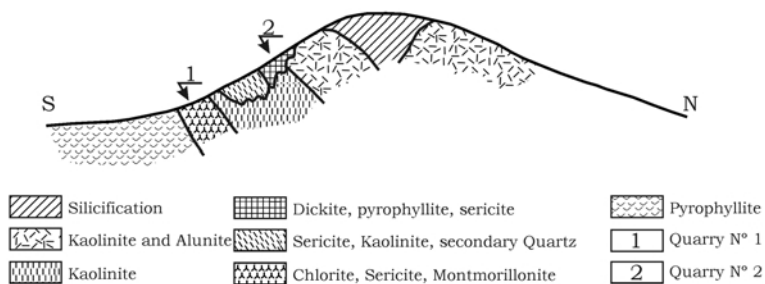

Fig. 2. Scheme of the Loma Blanca mine (after Hayase & Maiza, 1974).

components of the Los Menucos Group, of Triassic age; they are intruded by andesitic dykes of the Taquetren Formation. The field relations of these units have been obscured by tectonism, covered by recent sediments and masked by the mineralizing process.

SAMPLING

Twenty samples were collected from the propylitic zone (Fig. 3a) to the advanced argillic zone (Fig. 3b); two profiles were in the intermediate argillic alteration zone (samples 08 to 10 from bottom to top) and in the advanced argillic alteration zone (samples 16 to 20 from top to bottom).

ANALYTICAL METHODS

A petrographic and mineralogical study of representative samples from the different alteration zones was carried out. Texture, morphology and space relations between the different alteration minerals were studied. An Olympus B2-UMA trinocular petrographic microscope with a built-in Sony 151A video camera, a high-resolution monitor and Image-Pro Plus image processing software were used. The mineralogical composition of bulk samples was determined by an X-ray diffract-ometer, using Rigaku D-Max III, with Cu-$K\alpha$ radiation of wavelength λ = 1.54178 Å and a graphite monochromator operated at 35 kV and 15 mA. Diffractograms were recorded from 2° to 60°2θ. Chemical analyses of bulk samples for major, minor and trace elements were carried out by ICP at Activation Laboratories Ltd. (ACTLABS, Canada).

Kaolinite samples were selected for H and O isotope analyses. Stable isotope analyses were carried out at ACTLABS. Results are presented as ‰ deviation with respect to SMOW. The reproducibility of results is better than ±0.5‰ for O and ±10‰ for H.

RESULTS

X-ray diffraction

The minerals identified by X-ray diffraction (XRD) are listed in Table 1. When kaolinite and dickite are associated, it is very difficult to differentiate them by this method. The two triplets located between 34° and 40°2θ were studied in detail. Dickite appears in very small proportions compared with kaolinite in the samples of the advanced argillic alteration zone (Fig. 4). In this zone, besides alunite, diaspore at the top and pyrophyllite in the highest area of the profile (samples 16 and 17) were identified. These minerals are found in isolated masses within the area of greatest hydrothermal activity as relics of a first stage of higher pressure and temperature.

The characteristic diffraction patterns for each alteration zone are shown in Fig. 5. Figure 5a shows the propylitic alteration zone, where chlorite and scarce illite can be identified. Feldspar from the andesitic rock is still present. Figure 5b depicts the quartz-sericitic zone. The predominant alteration
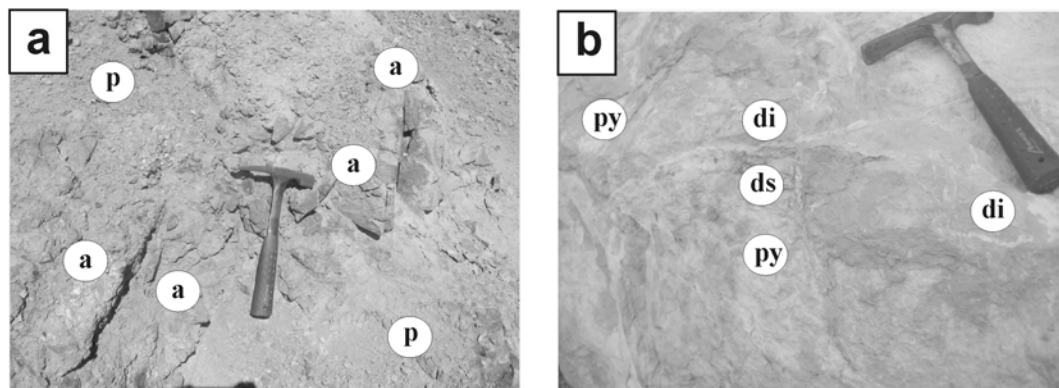

FIG. 3. (a) Propylitic alteration zone: a = andesite; p = propylitic area. (b) Advanced argillic alteration zone: di = dickite; py = pyrophyllite; ds = diaspore.

TABLE 1. Main minerals identified by XRD.

Sample	Clay minerals	Other minerals present	Alteration
01	Chlorite	Feldspar−quartz	Propylitic
02	Chlorite > illite	Feldspar−quartz	
03	Chlorite > illite	Feldspar−quartz	
04	Illite > chlorite	Feldspar - quartz	Sericitic
05	Illite	Quartz	
06	Kaolinite	Quartz	Intermediate
07	Kaolinite	Quartz	argillic
08	Kaolinite	−	
09	Kaolinite	Quartz	
10	Kaolinite	Quartz	
11	Kaolinite	Quartz	Silicified zone
12	Kaolinite	Quartz	
13	Kaolinite	Quartz	
14	Kaolinite > dickite	Natroalunite−quartz	Advanced argillic
15	Kaolinite > dickite	Natroalunite−diaspore−quartz	
16	Kaolinite > dickite−pyrophyllite	Natroalunite−quartz	
17	Kaolinite > dickite−pyrophyllite	Natroalunite−quartz	
18	Kaolinite > dickite	Natroalunite−quartz	
19	Kaolinite > dickite	Natroalunite−quartz	
20	Kaolinite > dickite	Natroalunite−quartz	

mineral is illite together with abundant quartz. Figure 5c shows the intermediate argillic alteration zone. Kaolinite and quartz reflections can be identified. The diffraction pattern of the silicified zone (Fig. 5d) is similar to that of Fig. 5c, but in the latter quartz predominates over kaolin. Figure 5e shows the characteristic minerals of the advanced argillic zone. Kaolinite, dickite, natroalunite, diaspore and quartz can be identified.

PETROGRAPHY

Propylitic alteration zone (samples 01 to 03)

The original texture is preserved. Plagioclase (andesine) crystals are altered, mainly to illite and calcite. Chlorites are found due to Fe availability. Plagioclase crystals of the groundmass are slightly more sodic, although they are still andesinic. Chlorite pseudomorphically replaces the mafic
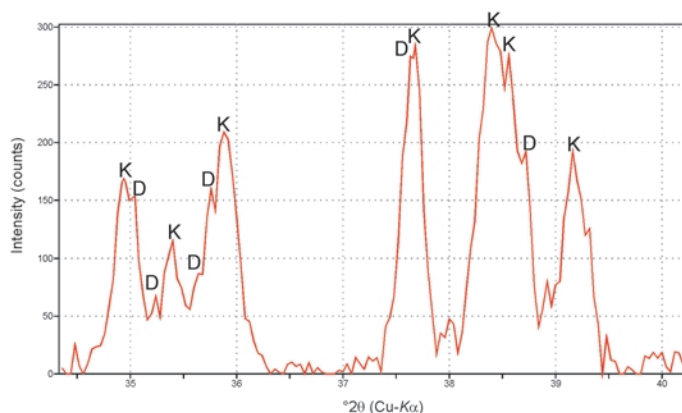

FIG. 4. Detail of the triplets located between 34 and 40º2$_y$ where kaolinite and dickite can be seen.
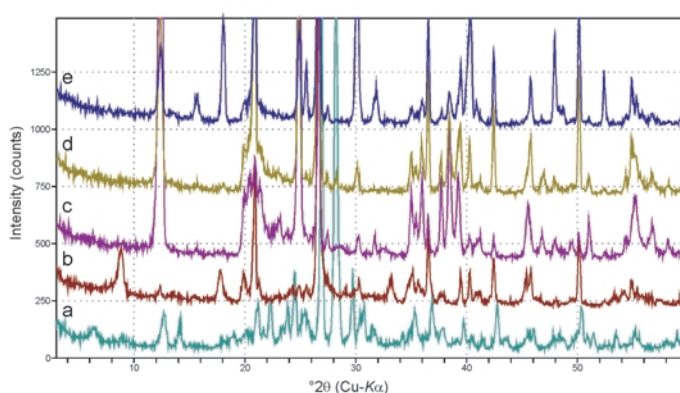
FIG. 5. Minerals of the different alteration zones identified by XRD. (a) Propylitic zone; (b) sericitic zone;
(c) intermediate argillic zone; (d) silicified zone; (e) advanced argillic zone.

minerals, and goethite is formed from the remaining Fe (Fig. 6A). Saccharoidal quartz is found as patches in the groundmass.

Two types of chlorites are recognized: a bluish low-pleochroic form (interpreted as rich-Mg, low-Al-type sheridinite) and the other, brownish grey, highly pleochroic, low interference colour, closely related to Fe oxides, thuringite (ripidolite).

Sericitic alteration zone (samples 04 and 05)

The andesitic tuff is highly altered. The ground-mass is completely argilized with secondary quartz. Iron oxides stain the whole rock (Fig. 6B). Sericite is the main alteration product. Quartz forms saccharoidal textures where three or more anhedral crystals are grouped. No original minerals are preserved.

Intermediate argillic alteration zone (samples 06 to 10)

The andesitic tuff is completely kaolinized. There is a stockwork of pure dickite veins, where the area between the veins is composed of a quartz-dickite association with variable amounts of illite-3T, and scarce Al hydroxides (diaspore). There are veins of dickite associated with boehmite crystals. A relic of highly altered, mainly silicified, host rock is found between the veins (Fig. 6C).

Silicified zone (samples 11 to 13)

Diaspore was positively identified in this zone and is closely related to dickite (Fig. 6D).

Advanced argillic alteration zone (samples 14 to 20)

This zone develops at the top of the hill coinciding with the greatest mineralization. The texture resembles that of tuff with lithic clasts replaced by natroalunite. There is no relict quartz. The groundmass is an association of quartz-kaolin and metallic minerals. Hydroxides of Al can be recognized in certain areas. Natroalunite is abundant in this area and is associated with dickite and pyrophyllite (Fig. 6E). Figure 6F shows diaspore twinned crystals, where kaolin has pseudomorphically replaced the core.

CHEMICAL COMPOSITION

Major elements analyses are shown in Table 2, and trace element contents are included in Table 3. Fe_2O_3, CaO, Na_2O and K_2O contents decrease from propylitic to advanced argillic alteration zones, whereas Al_2O_3 and LOI increase in the kaolinite-natroalunite zone.

Natroalunite was identified by XRD and with a petrographic microscope in samples 14 to 20. Natroalunite composition was determined by XRD using basal reflections (003, 006 and 009). Maiza & Mas, 1980, synthesized the minerals of the series from sericite alteration in a H_2SO_4 solution with varying amounts of KCl and NaCl. They determined the c_o values in each of the products obtained and checked them by chemical analysis. With these values they fitted a straight line by the least-squares method. The calculated value for natroalunite from
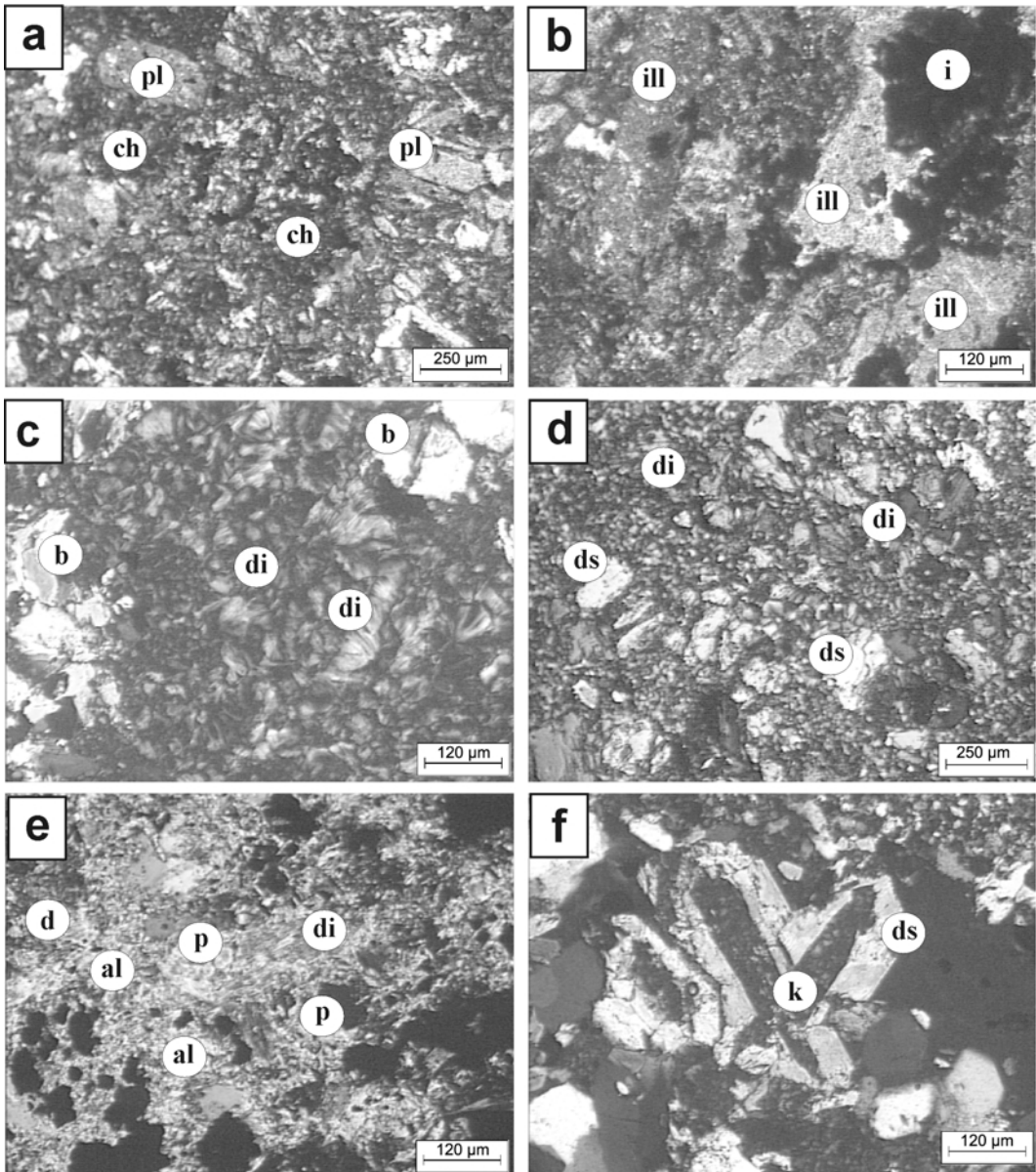
Fig. 6. (A) Propylitic zone: andesite texture is preserved. Plagioclase (pl) is altered to illite. Chlorites (ch) are abundant. (B) Sericitic zone: andesitic tuff is altered mainly to illite (ill). Fe oxides stain the whole rock (i). (Cc) Intermediate argillic alteration zone. Veins of dickite (di) are associated with boehmite crystals (b). (D) Silicified zone. Diaspore (d) is closely related to dickite (di). (E) Advanced argillic alteration zone: alunite (al) is associated with dickite (di) and pyrophyllite (p). (F) Diaspore twinned crystals (ds) have pseudomorphically replaced kaolin (k).

Loma Blanca is 16.83 Å, which corresponds to 87% Na. The formula calculated on this basis is $(Na_{0.13}K_{0.87})Al_3(SO_4)_2(OH)_6$. The percentage of this mineral, calculated from the S content, ranges between 2% and 25%. The sulphur content in samples 01 to 13 is attributed to the sulphides

TABLE 2. Chemical analyses of major elements in whole-rock samples from the Loma Blanca mine (wt.%).

Sample	SiO$_2$	Al$_2$O$_3$	Fe$_2$O$_3$	MnO	MgO	CaO	Na$_2$O	K$_2$O	TiO$_2$	P$_2$O$_5$	S	LOI	Total
01	60.22	17.35	6.55	0.075	1.43	1.20	5.42	0.96	0.790	0.29	0.04	5.16	99.45
02	58.82	17.08	5.10	0.083	2.11	2.86	5.26	1.00	0.744	0.25	0.05	5.47	98.78
03	57.74	17.84	5.43	0.060	1.89	2.11	5.74	0.91	0.803	0.27	0.04	5.58	98.38
04	62.3	17.28	7.05	0.497	0.78	0.44	0.26	2.28	0.718	0.24	0.04	6.91	98.77
05	63.14	16.08	9.45	0.027	0.39	0.24	0.52	3.01	0.933	0.35	0.21	6.17	100.30
06	51.08	32.52	0.35	0.002	0.03	0.13	0.07	0.15	0.554	0.19	0.23	12.85	97.93
07	59.01	28.39	0.11	<0.001	0.02	0.09	0.05	<0.01	0.737	0.17	0.16	10.89	99.46
08	44.88	38.68	0.12	<0.001	0.02	0.05	0.07	0.06	0.101	0.13	0.13	14.43	98.52
09	49.99	33.33	0.04	<0.001	0.14	0.08	0.37	0.13	0.913	0.21	0.26	13.23	98.42
10	60.9	27.05	0.11	0.005	0.03	0.06	0.12	0.33	0.954	0.20	0.43	10.64	100.40
11	65.93	18.85	4.73	0.001	0.07	0.22	0.25	0.79	0.910	0.30	0.24	8.79	100.80
12	67.08	21.43	0.13	<0.001	0.02	0.05	0.09	0.13	0.787	0.18	0.36	9.03	98.92
13	67.43	21.05	0.06	<0.001	0.01	0.97	0.09	0.14	0.755	0.16	0.33	9.12	99.78
14	56.87	17.35	3.96	0.001	0.09	0.57	1.09	0.59	0.854	0.25	3.68	16.38	98.00
15	64.18	16.28	5.04	<0.001	0.06	0.41	0.34	0.18	0.775	0.80	1.41	10.12	98.19
16	65.82	18.41	1.02	<0.001	0.02	0.11	0.63	0.41	0.931	0.22	1.94	11.80	99.38
17	54.68	20.34	0.96	<0.001	0.01	0.13	1.44	1.01	0.860	0.28	4.78	18.81	98.53
18	69.18	16.25	0.09	<0.001	<0.01	0.13	0.67	0.42	0.872	0.31	2.08	11.35	99.28
19	65.52	16.95	0.23	<0.001	0.03	0.11	0.69	0.45	0.871	0.21	2.70	15.91	101.00
20	34.02	37.82	0.22	<0.001	0.05	0.15	1.21	0.93	1.123	0.52	3.68	23.03	99.07

present (covellite, sphalerite and pyrite). Sulphides were identified with a petrographic microscope on polished sections in almost all the samples, so the total percentage of natroalunite is considered to be slightly smaller than the calculated value.

Large Ba, Sr, V and Zr contents were observed, mainly in intermediate argillic and advanced argillic zones. Co, Ni, Cu, Zn and Rb are more common in the propylitic zone. Be, Ge, In, Sn, Mo, Nb and Ag are insignificant in all the samples.

Ba + Sr $vs.$ Ce + Y + La, Fe$_2$O$_3$ + TiO$_2$ $vs.$ Cr + Nb and Zr $vs.$ TiO$_2$ plots are shown in Fig. 7.

The chondrite-normalized REE diagram according to Boynton, 1984 (Rollinson, 1992), for the samples of the propylitic and sericitic alteration zones are shown in Fig. 8a and b for the samples of intermediate and advanced argillic alteration zones. In the latter, especially in pure kaolin samples such as 08, there is marked $LREE$ impoverishment with respect to $HREE$, especially when compared with the less altered samples (Fig. 8a). There is no evidence of a positive Ce anomaly, which is typical of the deposits of residual and/or meteoric origin (Cravero et $al.$, 2001).

$LREE$ are more abundant than $HREE$ in the intermediate argillic alteration and advanced argillic alteration zones.

O and H isotopes

δ^{18}O and δD‰ values of kaolin samples from the Loma Blanca mine are shown in Table 4. δ^{18}O values in kaolinites range from 10.8‰ to 13.2‰, and δD from −83‰ to −85‰. Although these values are within the range of variation for hydrothermal kaolins (Murray & Janssen, 1984), they are larger than those determined for other deposits in the area (Blanquita and Equivocada mines, Marfil et $al.$, 2005), where O ranges between 4.8‰ and 10.3‰.

DISCUSSION

Cr and Nb contents are small, as occurs in kaolin deposits of hypogene origin (Dill et $al.$, 2000) (Fig. 7b). Kaolinites formed from hydrothermal alteration of acid-type igneous rocks show enrichment in Ba and Sr, whereas Cr, Nb, Ti and the lanthanides tend to concentrate in kaolinites formed from meteoric processes (Dill et $al.$, 1997). The large Ba + Sr contents in the kaolinized zone in the Loma Blanca mine (well above 1000 ppm) and the small Ce + Y + La contents (<100 ppm) (Fig. 7a) suggest a hypogene origin. Zr is a good indicator of the degree of meteorization of the parent rocks and Ti is a geochemically

TABLE 3. Chemical analyses of trace elements in samples from the Loma Blanca mine (ppm).

Sample	Sc	V	Ba	Sr	Y	Zr	Cr	Co	Ni	Cu	Zn	Ga	As
01	12	204	292	564	14	153	50	25	140	30	130	22	6
02	9	168	1106	503	14	178	<20	26	<20	10	130	22	<5
03	9	177	330	539	15	179	<20	26	<20	20	180	24	<5
04	11	214	948	92	13	159	<20	34	50	30	350	19	15
05	17	391	928	2301	47	127	120	6	20	70	40	25	12
06	5	147	217	2525	<2	121	30	<1	<20	<10	<30	26	10
07	5	131	166	1902	<2	123	<20	<1	<20	<10	<30	22	8
08	2	115	1109	1504	<2	58	30	<1	<20	<10	<30	32	13
09	5	149	577	2529	<2	156	30	<1	<20	10	<30	27	9
10	7	132	2727	1992	3	116	60	5	<20	20	40	23	5
11	8	277	626	1037	<2	180	<20	2	<20	10	<30	24	7
12	4	120	1743	2030	<2	160	<20	<1	<20	<10	40	12	11
13	5	129	864	1688	2	272	<20	<1	<20	<10	<30	13	12
14	6	317	1093	1740	5	150	30	<1	<20	<10	<30	18	9
15	6	232	5990	4765	<2	171	<20	<1	<20	<10	<30	22	13
16	10	178	585	1696	<2	244	40	<1	<20	<10	40	18	11
17	7	149	860	1766	<2	120	40	<1	<20	10	40	18	12
18	7	109	796	1918	<2	165	20	<1	<20	<10	<30	17	8
19	4	117	533	1756	<2	144	30	<1	<20	<10	<30	14	10
20	9	146	955	4499	2	192	50	<1	<20	60	<30	27	45

Table 3 (cont).

Sample	Rb	Nb	Mo	Ag	Sb	Hf	Ta	W	Tl	Pb	Bi	Th	U
01	26	6	7	5.1	5.5	4.0	0.4	<1	0.4	46	<0.4	4.2	1.1
02	24	6	2	2.7	6.6	4.6	0.4	<1	0.4	8	<0.4	5.0	1.2
03	25	7	3	1.7	6.3	5.4	0.4	<1	0.4	7	<0.4	5.4	1.3
04	73	6	7	1.7	5.2	4.6	0.4	<1	1.3	15	<0.4	5.4	2.3
05	95	5	3	<0.5	<0.5	3.5	0.3	2	0.6	14	<0.4	4.4	4.5
06	<2	4	<2	<0.5	6.4	3.1	0.2	<1	0.2	19	<0.4	3.1	1.2
07	<2	5	<2	<0.5	5.3	3.4	0.3	<1	<0.1	26	<0.4	3.6	0.6
08	<2	<1	<2	<0.5	6.7	1.4	<0.1	<1	<0.1	37	<0.4	2.3	0.3
09	<2	7	<2	<0.5	6.8	4.3	0.3	<1	<0.1	37	<0.4	4.0	0.7
10	6	6	<2	0.6	1.9	2.9	0.4	<1	0.1	36	<0.4	3.8	1.0
11	30	7	2	2.7	0.9	4.5	0.4	1	0.6	41	0.7	7.1	3.6
12	<2	5	<2	4.3	11.6	4.5	0.3	<1	<0.1	19	<0.4	4.0	1.0
13	<2	4	<2	0.7	6.7	7.1	0.2	<1	<0.1	16	<0.4	4.1	1.5
14	<2	4	4	1.7	15.2	4.0	0.2	2	<0.1	52	<0.4	5.9	2.2
15	6	5	6	6.9	11.0	4.9	0.2	2	0.2	191	0.6	24.6	5.8
16	<2	5	<2	1.8	7.0	6.3	0.3	1	<0.1	110	<0.4	4.7	1.6
17	<2	5	6	1.4	8.3	3.6	0.4	1	0.2	211	<0.4	5.5	1.4
18	<2	5	<2	1.3	1.8	3.9	0.4	1	<0.1	68	<0.4	6.3	1.3
19	<2	4	<2	4.0	10.3	4.0	0.2	<1	<0.1	158	<0.4	5.9	1.1
20	<2	7	4	5.2	5.1	4.5	0.4	2	<0.1	143	<0.4	11.1	1.7

immobile element under surface conditions. Therefore kaolins with large Zr and Ti contents indicate a near-surface formation environment. In Fig. 7c it can be seen that the contents of these elements in the Loma Blanca mine allow classification of these rocks as kaolins of hypogene origin. Likewise, Fe tends to be concentrated mainly during supergene processes. The Fe_2O_3 + TiO_2 content in this kind of deposit is above 1%. In Fig. 7b it can be seen that the content of these

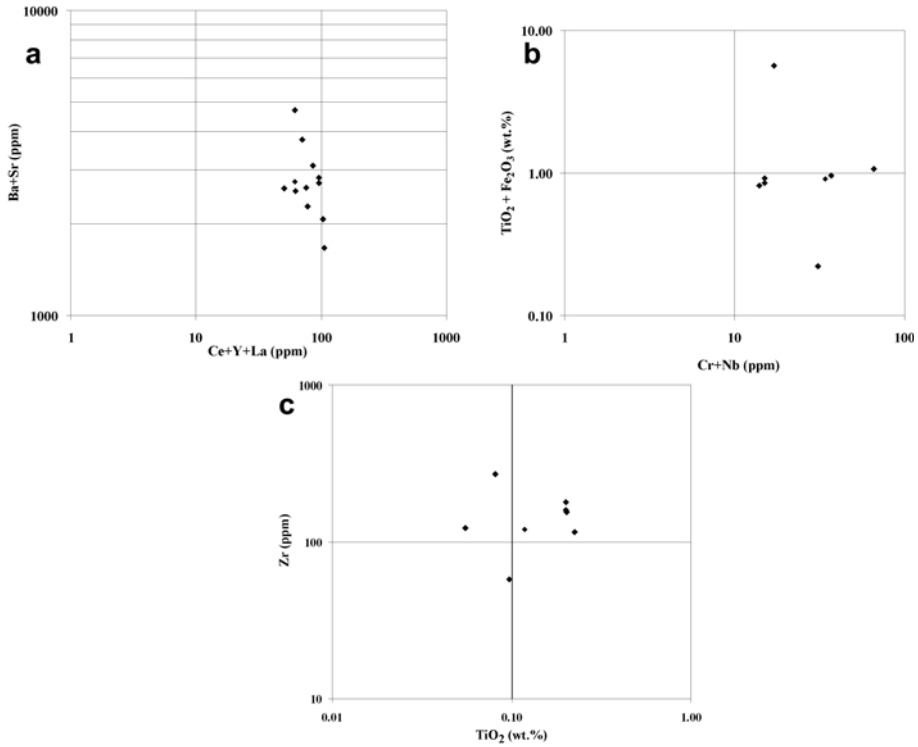FIG. 7. Data plot of samples from argillic zone. (a) Ba + Sr *vs.* Ce + Y + La. (b) Fe$_2$O$_3$ + TiO$_2$ *vs.* Cr + Nb. (c) Zr *vs.* TiO$_2$.

elements provides evidence for a hypogene origin. The large Fe$_2$O$_3$ content in sample 11 is attributed to the presence of pyrite, which was identified in polished sections.

Although the δ^{18}O values in kaolinites are large, they are within the ranges corresponding to hydrothermal kaolins. It is assumed that mixing with meteoric waters has occurred, which changed
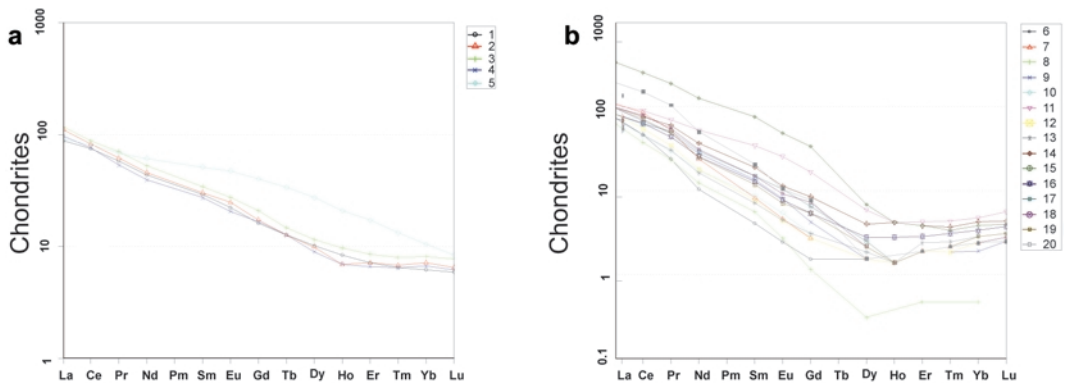
FIG. 8. (a) *REE* in the intermediate propylitic and sericitic alteration zones. (b) *REE* in the intermediate argillic alteration and advanced argillic alteration zones.

TABLE 4. δ^{18}O and δD ‰ values of kaolin samples from the Loma Blanca mine.

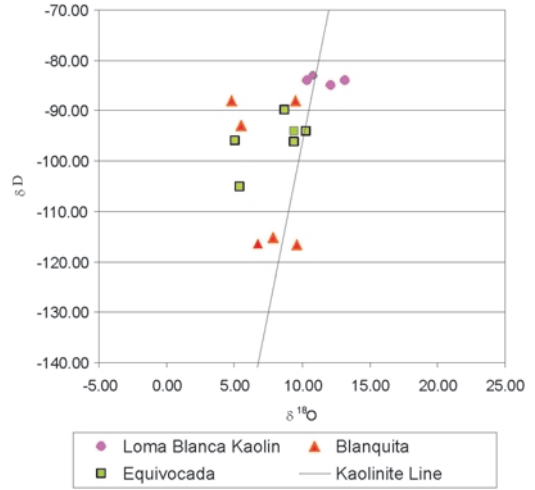| Sample	δ^{18}O$_{SMOW}$‰	δD$_{SMOW}$‰
6	10.8	−83
08	13.2	−84
09	12.1	−85
20	10.4	−843

FIG. 9. δ^{18}O and δD values in Loma Blanca kaolins are compared with those from the Blanquita and Equivocada mines.

the physicochemical conditions of the solutions. Evidence is provided by the relict morphology of diaspore and its hydration, which led to the formation of boehmite and to the residual form of pyrophyllite areas. The results of δ^{18}O and δD obtained for other deposits in the area (Blanquita and Equivocada mines) are compared with those of the Loma Blanca mine in Fig. 9.

A schematic summary of the paragenetic sequence is given in Table 5. The main Al minerals of higher temperature occur predominantly in the central area below the silicified zone, which is responsible for protecting the deposit from subsequent erosion processes. Dickite and nacrite frequently occur in deposits of hydrothermal

origin (Murray, 1988). Numerous authors have synthesized pyrophyllite at temperatures above 260ºC (Grim, 1969; Roy & Osborn, 1954; Hemley, 1959; Reed & Hemley, 1967; and Tzuzuki & Mizutani, 1971). The coexistence of

TABLE 5. Summary of the paragenetic sequence.

pyrophyllite and kaolinite allows estimating a maximum temperature of 350ºC.

Diaspore can be recognized frequently in kaolin deposits of hydrothermal origin. According to Roy & Osborn (1954), the boehmite-diaspore transformation temperature is between 270 and 300ºC at 175−1500 atm. water pressure.

CONCLUSIONS

(1) The mineral assemblage (dickite-natroalunite-pyrophyllite-diaspore), the alteration zonation pattern (laterally concentric), the geochemistry of trace elements, the relation between *LREE* and *HREE* and the small $\delta^{18}O$ values suggest that the Loma Blanca deposit was formed by hydrothermal processes.

(2) Mineralization developed in two stages: the first stage, of higher temperature, led to the formation of dickite, pyrophyllite and diaspore. Then the temperature decreased due to contamination with meteoric water, and alunite and kaolinite developed.

(3) The mineral assemblage allows estimating a formation temperature between 270 and 350ºC.

REFERENCES

Cravero F., Domínguez E. & Iglesias C. (2001) Genesis and applications of the Cerro Rubio kaolin deposit, Patagonia (Argentina). *Applied Clay Science*, **18**, 157−172.

Dill H (2001) The geology of aluminium phosphates and sulphates of the alunite group minerals: a review. *Earth Science Reviews*, **53**, 35−93.

Dill H.G., Bosse H.-R., Henning K.-H. & Fricke A. (1997) Mineralogical and chemical variations in hypogene and supergene kaolin deposits in a mobile fold belt-The Central Andes of northwestern Peru. *Mineralium Deposita*, **32**, 149−163.

Dill H., Bosse H.-R. & Kassbohm J. (2000) Mineralogical and chemical studies of volcanic-related argillaceous industrial minerals of the Central American Cordillera (Western El Salvador). *Economic Geology*, **95,** 517−538.

Ece Ö, Schroeder A.P., Smilley M.J. & Wampler J.M. (2008) Acid-sulphate hydrothermal alteration of andesitic tuffs and genesis of halloysite and alunite deposits in the Biga Peninsula, Turkey. *Clay Minerals*, **43**, 281−315.

Grim H. (1969) *Clay Mineralogy*. 2nd Edition. Pp. 131−137. McGraw Hill Book Co, New York, USA.

Hayase K. & Maiza P. (1974) Génesis del yacimiento de caolín de mina Loma Blanca, Los Menucos, Provincia de Río Negro, Argentina. *V Congreso Geológico Argentino*. Buenos Aires, Argentina, 139−151.

Hemley J.J. (1959) Some mineralogical equilibria in the system K_2O-Al_2O_3-SiO_2-H_2O. *American Journal of Science*, **257**, 241−270.

Labudia C. & Bjerg E. (1994) Geología del sector oriental de la hoja Bajo Hondo (39e), Provincia de Río Negro. *Revista de la Asociación Geológica Argentina*, **49**, 284−296.

Maiza P. (1972) *Los yacimientos de caolín originados por la actividad hidrotermal en lo principales distritos caoliníferos de la Patagonia, República Argentina.* PhD thesis, Universidad Nacional del Sur. Argentina.

Maiza P. & Mas G. (1980) Estudio de los sulfatos alunita−natroalunita. Síntesis de la serie. *Revista de la Asociación Argentina de Mineralogía, Sedimentología y Petrología*, **11**, 32-41.

Maiza P. & Mas G. (1981) Presencia de natroalunita en Mina Equivocada, Río Negro. Su significado. *8th Congreso Geologico Argentino*, San Luis, Actas IV, 285−292.

Maiza P.J., Pieroni D. & Marfil S.A. (2003) Geochemistry of the hydrothermal kaolins in the SE area of Los Menucos. Prov. de Río Negro. A clay odyssey. *Proceedings of the 12th International Clay Conference*. Argentina, 2001, Elsevier, 123−130.

Maiza P.J., Marfil S.A. & Montecchiari N. (2009) Alteration zonation 'Loma Blanca' kaolin deposit, Los Menucos, Rio Negro Province, Argentina. *XIV Internacional Clay Conference*, Abstracts Vol. **1**, p. 188.

Marfil S.A., Pieroni D. & Maiza P.J. (2000) Dickita y alunita en mina Blanquita. Los Menucos. (Province de Río Negro). *V Congreso de Mineralogía y Metalogenia. MINMET 2000*, La Plata. Argentina, 281−286.

Marfil S.A., Maiza P.J., Cardellach E.. & Corbella M. (2005) Origin of kaolin deposits in the 'Los Menucos', Río Negro Province, Argentina. *Clay Minerals*, **40**, 283−293.

Murray H. & Janssen J. (1984) Oxygen isotopes−indicators of kaolin genesis? *Proceedings of the 27th International Geological Congress*, **15**, 287−303.

Pandarinath K., Dulski P. Torres Alvarado I.S. & Verma S.P. (2008) Element mobility during the hydrothermal alteration of rhyolitic rocks of the Los Azufres geothermal field, Mexico. *Geothermics*, **37**, 53−72.

Pankurst R.J.C., Rapela W., Caminos R., Llambías E. & Parica C. (1992) A revised age for the granites of the central Somoncura Batholith, North Patagonian Massif. *Journal of South American Earth Sciences*, **5,** 321−325.

Papoulis D. & Tsolis-Katagas P. (2008) Formation of alteration zones and kaolin genesis, Limnos Island, northeast Aegean Sea, Greece. *Clay Minerals*, **43**, 631−646.

Papoulis D., Tsolis-Katagas P. & Katagas C. (2004). Monazite alteration mechanisms and depletion measurements in kaolins. *Applied Clay Science*, **24**. 271−285.

Reed B.L. & Hemley J.J. (1967) Ocurrence of pyrophyllite in Kekiktuk Conglomerate. Pp. 162−166 in: *Book Range, Northeastern Alaska.* U.S. Geological Survey.

Rollinson H. (1992) *Using geochemical data: Evaluation, presentation, interpretation.* University of Zimbabwe.

Roy R. & Osborn E. (1954) The system Al_2O_3-SiO_2-H_2O. *American Mineralogist*, **39,** 853−885.

Terakado Y. & Fujitani T. (1998) Behavior of the rare earth elements and other trace elements during interactions between acidic hydrothermal solutions and silicic volcanic rocks, southwestern Japan. *Geochimica et Cosmochimica Acta*, **62**, 1903−1998.

Tzuzuki Y. & Mizutani S. (1971) A study of rock alteration process based on kinetics of hydrothermal experiment. *Contributions to Mineralogy and Petrology*, **30**, 15−33.